SSRG International Journal of Electrical and Electronics Engineering
ISSN: 2348-8379/ https://doi.org/10.14445/23488379/IJEEE-V11I9P128

Volume 11 Issue 9, 316-325, September 2024


*Original Article*

# Design of a High-Gain MEMS-Based Microstrip Patch Antenna for RF Energy Harvesting in Millimeter-Wave 5G Applications

Redia Mohd Redzuwan[1,2*], Jahariah Sampe[1], Rhonira Latif[1], Zeti Akma Rhazali[3], Noor Hidayah Mohd Yunus[4]

[1]*Institute of Microengineering & Nanoelectronics, Universiti Kebangsaan Malaysia, Malaysia.*
[2]*Institute of Energy Infrastructure (IEI), Universiti Tenaga Nasional, Malaysia.*
[3]*Institute of Power Engineering (IPE), Universiti Tenaga Nasional, Malaysia.*
[4]*Advanced Telecommunication Technology, Communication Technology Section, Universiti Kuala Lumpur British Malaysian Institute, Malaysia.*

[*]*Corresponding author: redia@uniten.edu.my*

Received: 13 July 2024 Revised: 15 August 2024 Accepted: 13 September 2024 Published: 28 September 2024

***Abstract -*** *The evolution of wireless technology has spurred the development of the Internet of Things (IoT), wearable electronics, and Fifth Generation (5G) systems, often requiring remote sensors that face power supply challenges. Antennas capable of harnessing ambient Radio Frequency (RF) energy has garnered significant attention as a solution to power these sensors, providing an alternative to traditional batteries and solar cells, especially in areas with limited access to sunlight. This paper focuses on designing microstrip patch antennas specifically for capturing RF energy in 28 GHz millimeter-wave (mmWave) 5G networks. The antennas are developed using three distinct substrates: Rogers RT Duroid 5880 (RT-5880), porcelain, and borosilicate glass, each with a consistent thickness of 0.787 mm. The dielectric constants for RT-5880, porcelain, and borosilicate glass are 2.2, 5.6, and 4.4, respectively. The antennas' performance metrics, including return loss (S11), gain, bandwidth, and Voltage Standing Wave Ratio (VSWR), are simulated and evaluated via CST Microwave Studio. The simulation outcomes indicate that all proposed antennas achieve a bandwidth exceeding 0.5 GHz, with RT-5880 at 1.58 GHz, porcelain at 1.73 GHz, and glass at 0.95 GHz. The S11 parameter results show that RT-5880 has -16.4518 dB, porcelain -24.06 dB, and borosilicate glass -33.90 dB, which is a 34.65% improvement as compared to others. Furthermore, borosilicate glass has a higher gain of 7.017 dB, compared to 6.472 dB and 5.475 dB for RT-5880 and porcelain, respectively. The antenna using borosilicate glass shows the best potential for RF energy harvesting in mmWave 5G applications.*

***Keywords -*** *Microstrip patch antenna, MEMS, Millimeter-wave applications, RF energy harvesting, 5G applications.*

## 1. Introduction

Recent breakthroughs in wireless communication technologies have paved the way for significant developments such as the Internet of Things (IoT), Fifth Generation (5G) Wireless Systems, and advanced sensor applications [1]. These innovations, particularly the deployment of sensors in remote areas, have facilitated seamless wireless interactions but have also introduced challenges in providing reliable remote power sources. Traditional energy sources, like batteries, demand regular maintenance and replacement, and solar cells face efficiency drawbacks in low-light conditions due to their dependence on sunlight [2].

In this context, the omnipresent ambient Radio Frequency (RF) energy emerges as a viable alternative, offering a solution to these power constraints. This has led to a surge in research focused on developing antennas capable of harnessing ambient RF signals to power IoT sensors, leveraging energy from 5G wireless signals.

Despite the pervasive nature of RF signals from sources such as radio, television broadcasts, cellular services, and Wi-Fi, the power density of these signals is relatively low, typically ranging from 0.0002 to 1 μW/cm² [3]. This is modest compared to other energy scavenging methods like solar, mechanical, or thermal.

However, the ability of RF energy harvesting systems to capture signals in diverse settings, both indoors and outdoors, makes them particularly appealing for 5G wireless communication applications. Figure 1 effectively demonstrates the process of transforming captured energy into a regulated form within the power system, suitable for various application loads.

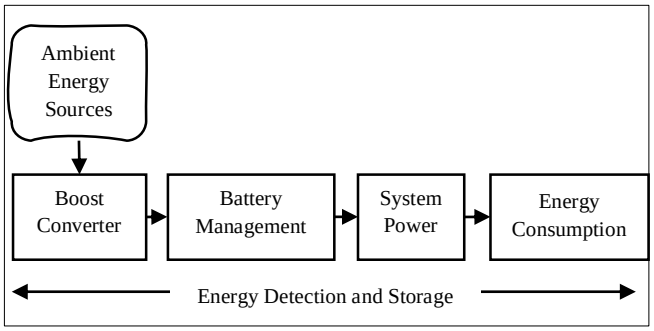


**Fig. 1 Commercial energy harvesting system**

The integration of Micro-Electromechanical Systems (MEMS) with RF components and circuits, known as RF MEMS technology, offers groundbreaking applications in various fields. Key among these are antennas, switches, filters, and wireless communication systems [4]. This technology stands out for its compactness and superior efficiency compared to conventional alternatives, enabling the consolidation of multiple functions onto a single chip. This not only shrinks the physical footprint of electronic devices but also significantly cuts down their production costs. The motivation for this paper is to design an RF MEMS-based antenna capable of capturing RF from 5G wireless signals. This antenna aims to power low-power IoT sensors, addressing a vital need in today's rapidly evolving digital landscape.

The recent decision by the Malaysian Communications and Multimedia Commission (MCMC) to allocate specific millimetre-wave (mmWave) frequency bands for 5G technology marks a significant development in telecommunications. Notably, the mmWave bands designated for this cutting-edge 5G technology fall between 26 and 28 GHz [5].

This frequency range, located at the higher end of the spectrum, has not been extensively utilized in comparison to the more commonly employed sub-6 GHz frequencies. One of the notable challenges with these higher mmWave frequencies is their increased vulnerability to atmospheric attenuation [6].

This issue primarily arises from the shorter wavelength characteristic of mmWave bands, which can lead to reduced signal strength and potentially affect the efficiency of 5G networks. To counteract this, employing antennas with higher gain levels has been identified as an effective strategy to mitigate the issues related to air attenuation.

Over the years, many papers have been published proposing antenna designs that meet a variety of objectives for application in RF energy harvesting, such as the dipole, monopole, Microstrip Patch Antenna (MPA), horn antenna, parabolic antenna, and so on. Some of the overviews can be found in [7]. Each of these antenna types has advantages and disadvantages based on the needs of the designer. Among the various antennas listed before, MPA is recommended for use in RF energy harvesters because of its small size, light weight, and ease of integration into portable devices, which make them suited for 5G applications [8].

A primary challenge with MPAs is their limited bandwidth and relatively low gain [9]. However, these limitations can be mitigated by employing a thicker substrate to increase surface wave radiation from the patch [10]. The material used for the substrate significantly affects the antenna's overall efficiency and execution. Typically, substrates with greater thickness and lower dielectric constants tend to improve antenna performance. This highlights the necessity of understanding how different substrate properties can impact design accuracy.

Designing millimeter-wave Microstrip Patch Antennas (MPAs) using commercial substrates like FR-4 poses several key challenges. FR-4, being a widely used and cost-effective material, has relatively high dielectric losses and a low dielectric constant, which can negatively impact the performance of MPAs at higher frequencies. These limitations result in higher signal attenuation and reduced efficiency, making FR-4 less suitable for millimeter-wave applications where precision and performance are critical. Additionally, FR4 substrates can exhibit significant variations in dielectric properties across different batches, leading to inconsistent antenna performance and manufacturing challenges.

Switching to porcelain and borosilicate substrates for millimeter-wave MPAs offers notable advantages. Porcelain and borosilicate glasses have superior dielectric properties, including lower dielectric losses and dielectric constants, which contribute to better signal propagation and reduced attenuation. These materials also provide better thermal stability and mechanical strength, ensuring consistent performance and durability under varying environmental conditions.

The use of glass substrates, such as borosilicate, can further enhance the integration of MPAs with other electronic components due to their excellent chemical resistance and compatibility with advanced fabrication techniques, thereby improving overall device performance and reliability in high-frequency applications.

The goal of this study is to fill in a gap in existing studies by exploring the use of glass-based substrates, including porcelain and borosilicate, for MPAs operating at higher frequencies, particularly in millimeter-wave 5G applications. The study involves designing a rectangular MPA operating at 28 GHz using these glass-based substrates for RF energy harvesting. The conventional RT-5880 substrate will also be used as a reference for comparison.

This study is intended to improve the performance of MPAs on glass substrates in high-frequency applications, which is critical for developing effective and affordable RF energy harvesting devices for 5G networks. The focus is on designing microstrip patch antennas at a frequency of 28 GHz for RF energy harvesting in millimeter-wave 5G systems, utilizing three different substrates: RT-5880, porcelain, and borosilicate glass. The performance of these antennas, including Voltage Standing Wave Ratio (VSWR), gains, return loss (S11), and bandwidth, will be assessed through CST software simulations.

The structure of this paper is as follows: A summary of previous studies on microstrip patch antennas using RT-5880, porcelain, and borosilicate glass substrates for mmWave 5G applications is presented in Section 2. Section 3 provides a detailed explanation of the antenna design. The findings, analysis, and discussion are presented in Section 4. Lastly, Section 5 summarizes the work and makes recommendations for further research.

## 2. Related Work

MPAs are one of the many types of antennas. They are becoming increasingly popular in wireless applications due to their small size, lightweight, cost-effectiveness, and simple fabrication [11]. Figure 2 illustrates the structure of a simple rectangular patch antenna. The Microstrip Patch Antenna (MPA) comprises four main components: the microstrip feed line, patch, substrate, and ground plane [12]. The radiating patch is placed on a dielectric substrate, with the ground plane on the opposite side. Typically made from conductive materials such as copper, both the radiating patch and the feed lines are mounted on the dielectric substrate. Photoetching is used to create the radiating patch and feed lines on the substrate.

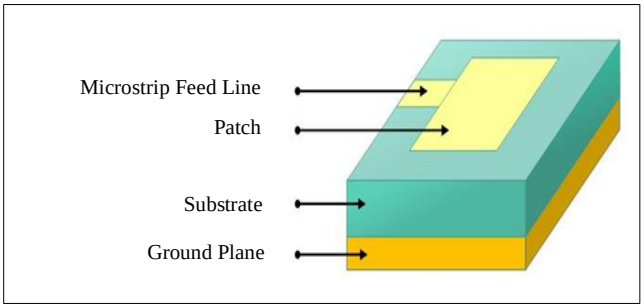


**Fig. 2 Simple rectangular patch antenna structure**

Another advantage of the MPA is that it can be designed in any shape, such as rectangular, circular, square, dipole, triangular or any other configuration, as shown in Figure 3 [13]. Rectangular and circular patches, in contrast, are highly favored because they are simple to analyze and fabricate. Additionally, they offer desirable radiation properties, particularly with minimal cross-polarization radiation [14, 15]. Considering these factors, the primary shape of the antenna used in this work will be a rectangular MPA.

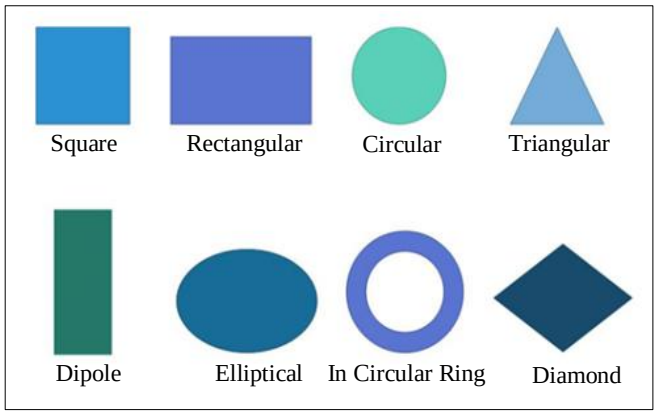


**Fig. 3 Geometries of patch antenna [16]**

Numerous researchers have explored the use of the RT-5880 substrate in designing 28 GHz microstrip patch antennas. For instance, [17] developed a rectangular MPA featuring vertical and horizontal slits using RT-5880 material with a thickness of 0.5 mm. The integration of slits was aimed at enhancing the antenna's bandwidth and gain, achieving a gain of 6.35 dBi and a bandwidth of 1.23 GHz. The study conducted by [18] involved the design of three distinct MPAs circular, triangular, and rectangular for 5G wireless communication applications at 28 GHz, employing RT-5880 with a 2.2 dielectric constant and 0.2mm thickness. The rectangular antenna demonstrated a return loss of -6.04dB, resonating at 27.85 GHz, while the circular and triangular designs resonated at 27.58 GHz and 26.8 GHz, respectively. However, this study did not disclose details on bandwidth and VSWR.

In [19], three compact rectangular MPAs were designed using RT-5880, R03003 and FR-4 substrates, each with a 0.5 mm thickness. These antennas, designed for 5G applications at 26 GHz, were investigated both with and without the integration of an Artificial Magnetic Conductor (AMC). Addressing the limitations of narrow bandwidth and low gain, the proposed RT-5880 patch antenna with AMC exhibited improved performance, resonating at 26.00 GHz with a broader bandwidth ranging from 25.70 GHz to 26.60 GHz.

In [20], a rectangular ring antenna incorporating a fork-shaped strip was designed to function at 26 GHz, addressing the 5G frequency range from 26.5 GHz to 40 GHz and achieving excellent gain performance. The design employed three distinct substrates: FR4, RT-5880, and R03003, each with a uniform thickness of 1.6 mm. The use of the RT3003 substrate in the proposed antenna design resulted in enhancements in return losses and overall gain. The design attained a peak gain of 6.76 dB.

In recent years, research on using porcelain and borosilicate substrates for millimeter-wave Microstrip Patch Antennas (MPAs) has been limited. Nevertheless, the author in [21] presented a 2.34 GHz hexagonal patch antenna that used a porcelain dielectric substrate. This antenna's performance was compared with that of an antenna using a lead glass dielectric substrate.

The hexagonal patch antenna made with a porcelain dielectric material exhibited significantly better gain performance than the one utilizing lead glass. In particular, the gain for the porcelain-based antenna was measured at 6.631 dB, whereas the lead glass-based antenna showed a gain of 5.566 dB. Simulation results validate that the hexagonal patch antenna with a porcelain dielectric outperforms the lead glass version in terms of gain. This indicates that porcelain could be a highly effective substrate for MPAs.

Similarly, [22] focused on designing antennas optimized for 5 GHz RF energy capture using Pyrex glass. The resultant antenna exhibited a bandwidth of 0.34 GHz and a gain of 5.022 dB, suggesting the feasibility of glass substrate as a substrate for MPAs. This study aims to enhance the performance of rectangular MPA on glass substrates for mm-wave 5G applications, which is crucial for creating efficient RF energy harvesting devices. It focuses on designing MPAs at 28 GHz for RF energy harvesting in millimeter-wave 5G systems using three substrates: RT-5880, porcelain, and borosilicate glass.

## 3. Antenna Design

When designing a rectangular microstrip patch antenna, three fundamental parameters must be carefully considered. These parameters include the operating frequency, the dielectric constant of the substrate, and the height of the dielectric substrate. In the case of the proposed antenna, three fundamental parameters are defined as follows:

1. Operating frequency, $f_o$*:* The design's resonant frequency is set at 28 GHz, aligning with the MCMC allocation of the 26 to 28 GHz frequency bands for 5G deployment in Malaysia.
2. Dielectric constant of the substrate, $\varepsilon_r$: Opting for a substrate with a higher dielectric constant is advantageous as it leads to more compact antenna dimensions.
3. Dielectric substrate, $h$*:* For energy harvesting applications, a smaller antenna size is preferred. Hence, a standard substrate height of 0.787 mm is selected for all substrates to facilitate performance comparison.

This paper provides a comparative analysis of three MPAs using different dielectric substrates: RT-5880, porcelain, and borosilicate glass. These substrates were chosen due to their significant impact on antenna performance. The main goal was to develop antennas capable of functioning at 28 GHz, adhering to performance standards. These include achieving a VSWR of 2 dB or less, a return loss (S11) below -10 dB, a line impedance matched to 50 Ohms, a bandwidth of at least 0.3 GHz, and a gain exceeding 5 dB, as detailed in Table 1 below.

**Table 1. Design specifications of the proposed antennas**

| Specifications | Values |
|---|---|
| Operating Frequency, $f_o$ | 28 GHz |
| Return Loss, S11 | Less than − 10dB |
| VSWR | ≤ 2 |
| Input Impedance, Z | 50 Ohms |
| Bandwidth | ≥ 0.3 GHz |
| Substrate thickness, h | 0.787 mm |
| Gain | ≥ 5 dB |

For this study, a rectangular MPA has been designed employing a microstrip feed line. For the construction of the patch, ground plane, and microstrip feeding line, Copper (Cu) has been chosen for its superior electrical conductivity and reliability. The specific dimensions and shape of the proposed antennas are clearly shown in Figure 4.

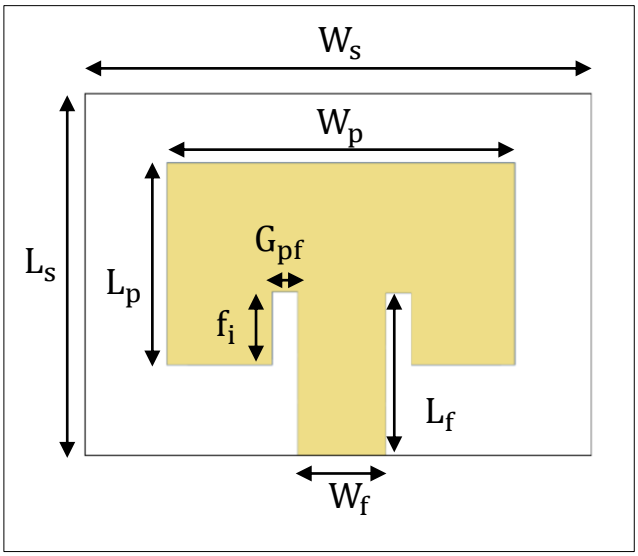


**Fig. 4 Dimensions and shape of the proposed patch antenna**

The design parameters for rectangular microstrip patch antennas are calculated based on known values of the resonant frequency,$f_o$ and dielectric constant (relative permittivity), $\varepsilon_r$ using the equations listed below [23].

The patch width, $W_p$ of the proposed antenna is determined using the widely used MPA equations shown below [24]:

$$W_p = \frac{c}{2f_r}\sqrt{\frac{2}{\epsilon_r+1}} \quad (1)$$

Where, c is the speed of light (3 x $10^8$ $ms^{-1}$), $f_r$ is the resonating frequency.

Equation (2) to Equation (5) are used to compute the length L of a rectangular patch. In practical scenarios, the electric field of an antenna extends beyond the physical dimensions of its length and width due to the fringing effect. The effective dielectric constant $\epsilon_{eff}$ evolves:

$$\epsilon_{eff} = \frac{\epsilon_r+1}{2} + \frac{\epsilon_r+1}{2}\left(1 + 12\frac{h}{W}\right)^{-1/2} \quad (2)$$

The actual length of the antenna design or effective patch length, $L_{eff}$. It comprises the antenna length multiplied by two, as given by:

$$L_{eff} = \frac{c}{2f_r\sqrt{\epsilon_{eff}}} \quad (3)$$

As a result of the fringing effect occurring at the edges or ends of the patch, an additional length is required. This increase in patch length is needed to consider the fringing effect. The length due to fringing effects $\Delta L$ can be defined as:

$$\Delta L = 0.412h\,\frac{(\epsilon_{eff}+0.3)\left(\frac{W}{h}+0.264\right)}{(\epsilon_{eff}-0.258)\left(\frac{W}{h}+0.8\right)} \quad (4)$$

Where, $h$ is the substrate thickness, as illustrated in Figure 2.

Thus, the length of the patch antenna is given by:

$$L_p = L_{eff} - 2\Delta L \quad (5)$$

The substrate width $W_s$ and the ground plane width $W_g$ is computed by:

$$W_s = W_g = 6h + W \quad (6)$$

The substrate length $L_s$ and the ground plane length $L_g$ is given by:

$$L_s = L_g = 6h + L \quad (7)$$

The sizes of the three antennas were calculated using Equations (1) - (7) mentioned earlier. To ensure consistent performance evaluation, all antennas in this study were designed with a standard thickness of 0.787 mm. The dielectric constant of the first antenna was 2.2, and an RT-5880 substrate was used. The second employed porcelain substrates with a dielectric constant of 5.6, while the third utilized borosilicate glass substrates with a dielectric constant of 4.4. However, the computed results did not match the intended 28 GHz frequency because the equations yielded only estimated values. Adjustments were needed to reach the target frequency, specifically by shortening the patch length to raise the frequency. The refined dimensions of the antennas, utilizing three distinct substrates, RT-5880, porcelain, and borosilicate glass, are detailed in Table 2.

**Table 2. Optimized parameter values of the three proposed antenna**

| Parameters | Value (mm) | | |
|---|---|---|---|
| | **RT-5880** | **Porcelain** | **Borosilicate Glass** |
| Ground Width, $W_g$ | 10.00 | 8.89 | 11.00 |
| Ground Length, $L_g$ | 13.56 | 14.00 | 14.73 |
| Patch Width, $W_p$ | 5.00 | 4.44 | 5.50 |
| Patch Length, $L_p$ | 6.78 | 7.00 | 7.36 |
| Substrate Width, $W_s$ | 10.00 | 8.89 | 11.00 |
| Substrate Length, $L_s$ | 13.56 | 14.00 | 14.73 |
| Feed Line Length, $L_f$ | 3.98 | 4.11 | 4.28 |
| Feed Line Width, $W_f$ | 1.11 | 1.11 | 1.11 |
| The gap between the patch and feed line, $G_{pf}$ | 0.50 | 0.50 | 0.50 |
| The distance inset feed, $F_i$ | 0.60 | 0.60 | 0.60 |

## 4. Results and Discussion

The simulations for all three suggested designs were carried out using the parameter values specified in Table 2. In the frequency ranges from 26 to 30 GHz, several antenna parameters, including return loss (S11), bandwidth, VSWR, radiation pattern, and gain, were examined. The next three sections provide further details regarding these findings.

### *4.1. Return Loss (S11) and VSWR*

Figure 5 illustrates the Return Loss (S11) for RT-5880, porcelain, and borosilicate glass. The simulation outcomes clearly indicate that all three optimized antennas resonate at 28.00 GHz, corresponding to a reference level of -10 dB. RT-5880 attained an S11 value of -16.4518 dB and a bandwidth of 1.58 GHz. Porcelain substrate had the lowest S11 value of -24.06 dB among the proposed antennas, but it had a maximum bandwidth of 1.7343 GHz. In contrast, borosilicate glass, with an S11 value of -33.90 dB, showed the highest value with a bandwidth of 0.95 GHz recorded.

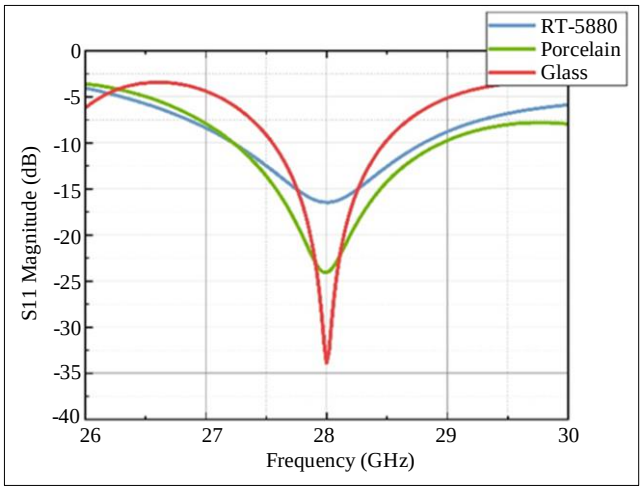


**Fig. 5 Simulated return loss for RT-5880, porcelain, and borosilicate glass**

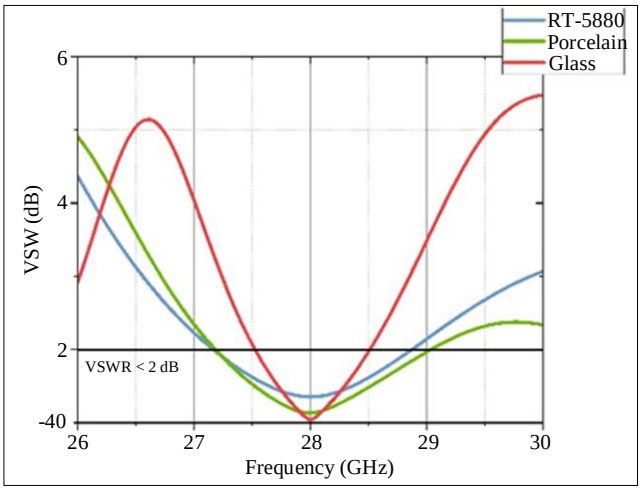


**Fig. 6 Simulated VSWR for RT-5880, porcelain, and borosilicate glass**

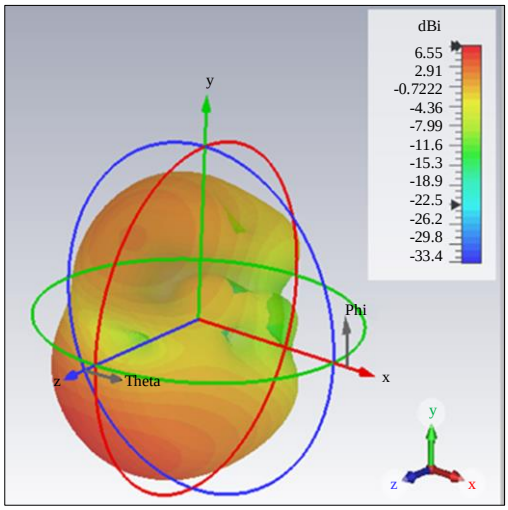


**(a)**

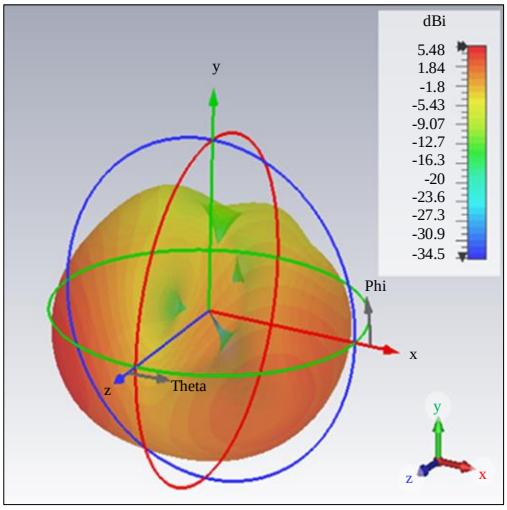


**(b)**

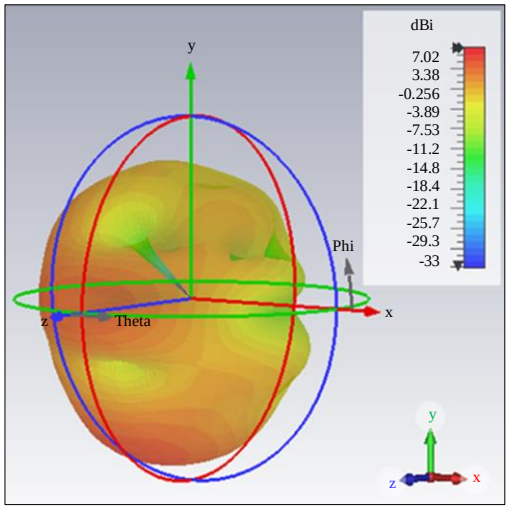


**(c)**

**Fig. 7 The Radiation pattern (a) RT-5880, (b) Porcelain, and (c) Borosilicate glass.**

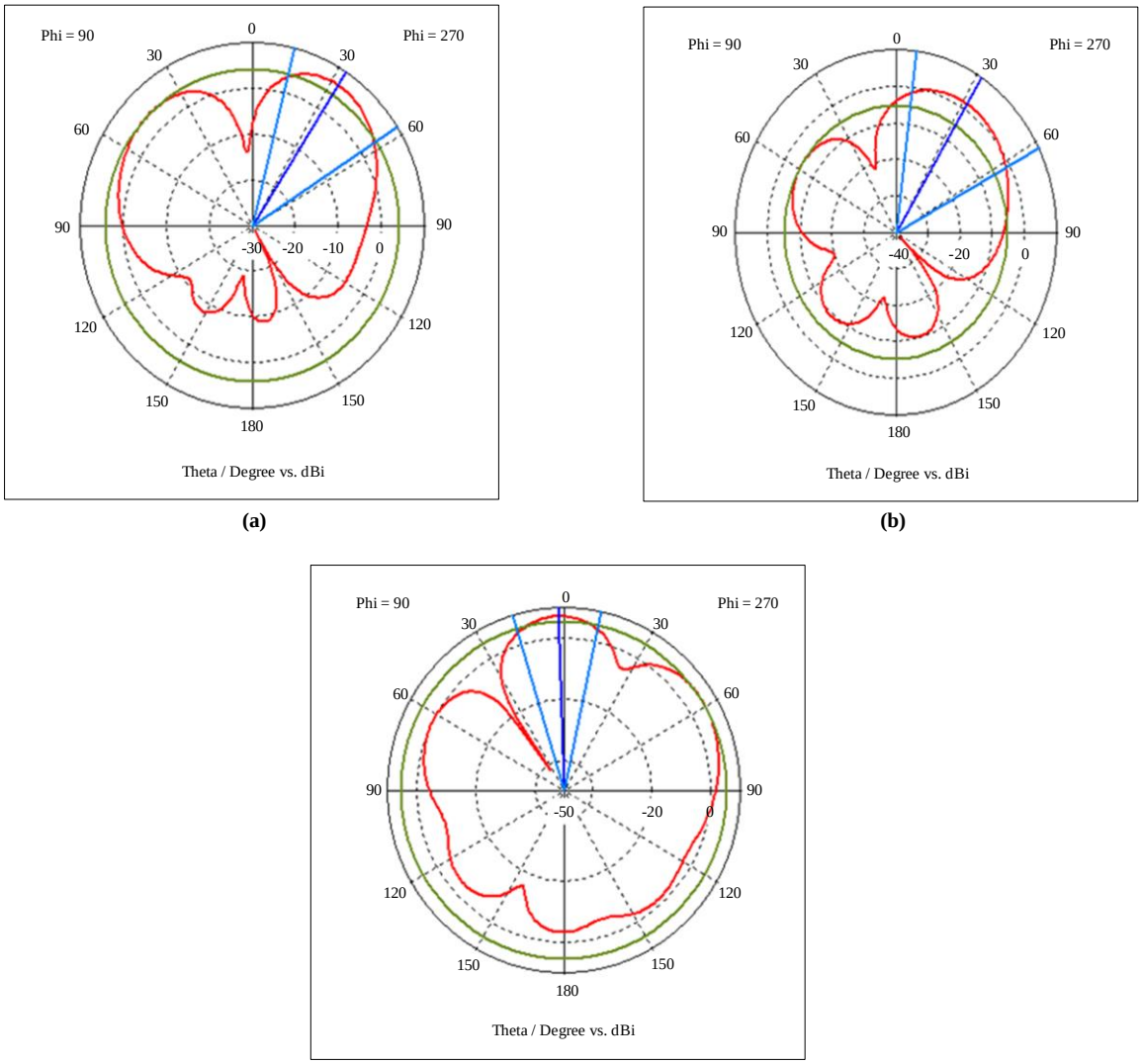


**Fig. 8 A two-dimensional (2D) illustration of the radiation patterns for (a) RT-5880, (b) Porcelain, and (c) Borosilicate glass.**

Despite the bandwidth not being exceptionally broad, it is considered adequate for the RF energy harvesting needs of the 5G applications addressed in this research, where gain and directivity are of higher importance. Another crucial parameter involves evaluating the alignment between the antenna's impedance and that of the connected transmission line.

The VSWR serves as an indicator of the efficiency of RF power transfer through the transmission line, ensuring a smooth transition from the source power to the load. The simulated VSWR values are shown in Figure 6, where the VSWR for RT-5880, porcelain, and borosilicate glass at 28.00 GHz were 1.3, 1.13, and 1.04, respectively. Since the ideal VSWR is usually designed to be less than or equal to 2, this result is quite good. All three of the suggested antennas meet the requirements to be used in 5G networks, as per ITU specifications.

### *4.2. Radiation Pattern*

The radiation pattern was further investigated with CST software, a critical aspect in the design and analysis of antennas as it directly influences their performance. Figure 7 presents a radiation pattern, along with the gains achieved by RT-5880, porcelain and borosilicate glass. The lowest gain was achieved by porcelain at 5.475 dB, followed by RT-5880 at 6.551 dB, and borosilicate glass achieved the highest gain of 7.017 dB.

High gain is desirable for antennas as it enhances their capability to efficiently capture RF energy from the surroundings and convert it into electrical power. Figure 8 shows the two-dimensional (2D) radiation patterns for antennas with RT-5880, porcelain, and borosilicate glass substrates. Radiation patterns are a critical aspect of antenna design and analysis because they visually represent the distribution of radiated power from an antenna.

The findings revealed that all three suggested antennas exhibit linear, directed behavior. This indicates that the antennas are designed to concentrate their energy in a specific direction, making them ideal for applications requiring long-range communication in that direction. It also suggests that the antennas achieve maximum radiation coverage from the observed omnidirectional pattern.

### *4.3. Comparative Analysis of the Suggested Antenna with other Works*

Table 3 compares the performance of three suggested antennas with other published references MPAs documented in the literature, focusing on variations in dielectric substrates: RT-5880, porcelain, and borosilicate glass. The return loss (S11) parameter, which is indicative of the antenna's efficiency in radiating the desired signal, shows a variation across the table, with the borosilicate glass MPA in this paper achieving an exceptionally low return loss of -33.90 dB, suggesting a highly efficient design. At 28.00 GHz, the current study demonstrates a marked gain enhancement using porcelain and borosilicate glass, achieving gains of 6.472 dB and 7.017 dB, respectively. These values surpass the previously reported maximum gain of 6.35 dB. This improvement is attributed to borosilicate glass's lower dielectric constant, which enhances antenna performance compared to materials like RT-5880 and porcelain substrates.

While there is a modest trade-off in the form of reduced bandwidth, with the borosilicate glass MPA achieving only 0.95 GHz, this narrower bandwidth helps to reject unwanted signals and maximize energy transfer. The lower dielectric constant of borosilicate glass results in superior gain and improved outcomes compared to the latest techniques reported in the literature, consequently enhancing overall device performance and reliability in high-frequency applications.

Considering the comparative outcomes, the use of borosilicate glass, characterized by its lower dielectric constant, leads to significant improvements in gain and return loss compared to RT-5880 and porcelain substrates. This results in better overall device performance and reliability in high-frequency applications, particularly in 5G technology. Despite the trade-off in bandwidth, the enhanced efficiency and gain position borosilicate glass MPAs are promising candidates for 5G systems.

By leveraging the unique properties of borosilicate glass, this study demonstrates that the proposed antennas offer superior performance metrics, making them highly suitable for integration into next generation 5G applications. The analytical comparison underscores the potential of borosilicate glass as an optimal substrate material for mmWave applications in microstrip patch antennas.

**Table 3. Comparison of the proposed antennas with other works**

| Author, Year | Dielectric Substrate | Type of Antenna | Operating Frequency (GHz) | Return Loss, S11 (dB) | Bandwidth (GHz) | Gain (dB) |
|---|---|---|---|---|---|---|
| [21] | Porcelain | Hexagonal Patch Antenna | 2.5 | -25 | Not available | 6.631 |
| [22] | Borosilicate Glass | Rectangular MPA with U slot | 5 | -17.655 | 0.34 | 5.359 |
| [18] | Rogers RT Duroid 5880 | Rectangular, Triangular, Circular MPA | 27.85, 26.8, 27.58 | -6.04, -23.2, -5.2 | Not available | 4.71, 4.74, 4.757 |
| [17] | Rogers RT Duroid 5880 | Rectangular MPA with Vertical and Horizontal Slits | 28.00 | -23.6 | 1.23 | 6.35 |
| This work | RT-5880 | Rectangular MPA | 28.00 | -16.4518 | 1.58 | 6.472 |
| This work | Porcelain | Rectangular MPA | 28.00 | -24.06 | 1.73 | 5.475 |
| This work | Borosilicate Glass | Rectangular MPA | 28.00 | -33.90 | 0.95 | 7.017 |

## 5. Conclusion

In this study, a rectangular microstrip patch antenna was designed for millimeter-wave 5G RF energy harvesting at 28 GHz, employing RT-5880, porcelain, and borosilicate glass substrates. Comprehensive analyses revealed that each of the proposed antenna designs successfully met key performance criteria, notably achieving a Voltage Standing Wave Ratio (VSWR) of 2 or less, a return loss below -10 dB, bandwidths of at least 0.3 GHz, and a minimum gain of 5 dB. Among these, the antenna with the borosilicate glass substrate stood out, registering a remarkable 34.65% improvement in the S11 parameter despite a reduction in bandwidth to 0.95 GHz, which aided in filtering out extraneous signals and enhancing the efficiency of energy transfer. Furthermore, it exhibited

superior performance in terms of gain, achieving 7.017 dB, in contrast to 6.472 dB with RT-5880 and 5.475 dB with porcelain. These results position the borosilicate glass-based antenna as a viable option for the front-end component of an integrated RF energy harvesting system. Future research could enhance these antennas by incorporating slots in the patch or using antenna arrays. Such modifications aim to improve various radiation characteristics, especially bandwidth, offering promising directions for advancing 5G RF energy harvesting technologies.

## Funding Statement

This work is funded by the PAME SDN BHD UKM Industry grant and UNITEN BOLD 2023 grant under the grants RR-2022-001 and J510050976, respectively.

## References

[1] Corina Covaci, and Aurel Gontean, "Piezoelectric Energy Harvesting Solutions: A Review," *Sensors*, vol. 20, no. 12, 2020. [CrossRef] [Google Scholar] [Publisher Link]

[2] D.M. Motiur Rahaman et al., "An Architecture of ULP Energy Harvesting Power Conditioning Circuit Using Piezoelectric Transducer for Wireless Sensor Network: A Review," *Asian Journal of Scientific Research*, vol. 8, no. 1, 2015. [CrossRef] [Google Scholar] [Publisher Link]

[3] Husam Hamid Ibrahim et al., "Radio Frequency Energy Harvesting Technologies: A Comprehensive Review on Designing, Methodologies, and Potential Applications," *Sensors*, vol. 22, no. 11, 2022. [CrossRef] [Google Scholar] [Publisher Link]

[4] Vijay K. Varadan, K.J. Vinoy, and K.A. Jose, *RF MEMS and Their Applications*, John Wiley & Sons Ltd., 2002. [CrossRef] [Google Scholar] [Publisher Link]

[5] A.K.M. Zakir Hossain et al., "A Planar Antenna on Flexible Substrate for Future 5g Energy Harvesting in Malaysia," *International Journal of Advanced Computer Science and Applications*, vol. 11, no. 10, pp. 151-155, 2020. [CrossRef] [Google Scholar] [Publisher Link]

[6] Dalia Nandi, and Animesh Maitra, "Study of Rain Attenuation Effects for 5G Mm-Wave Cellular Communication in Tropical Location," *IET Microwaves, Antennas & Propagation*, vol. 12, no. 9, pp. 1504-1507, 2018. [CrossRef] [Google Scholar] [Publisher Link]

[7] Ranjan Mishra, "An Overview of Microstrip Antenna," *HCTL Open International Journal of Technology Innovations and Research (IJTIR)*, vol. 21, no. 2, pp. 1-17, 2016. [Google Scholar]

[8] Hirendra Das, Mridusmita Sharma, and Qiang Xu, "Microstrip Antenna: An Overview and Its Performance Parameter, Latest Trends in Design and Application," *Smart Antennas*, pp. 3-14, 2022. [CrossRef] [Google Scholar] [Publisher Link]

[9] Zain U. Abedin, and Zahid Ullah, "Design of a Microstrip Patch Antenna with High Bandwidth and High Gain for UWB and Different Wireless Applications," *International Journal of Advanced Computer Science and Applications*, vol. 8, no. 10, pp. 379-382, 2017. [CrossRef] [Google Scholar] [Publisher Link]

[10] Nurulazlina Ramli et al., "Design and Performance Analysis of Different Dielectric Substrate Based Microstrip Patch Antenna for 5G Applications," *International Journal of Advanced Computer Science and Applications*, vol. 11, no. 8, pp. 77-83, 2020. [CrossRef] [Google Scholar] [Publisher Link]

[11] Shilpee Patil, Binod Kumar Kanaujia, and Anil Kumar Singh, *Basic Theory and Design of Printed Antennas*, Printed Antennas, 1st ed., CRC Press, 2020. [Google Scholar] [Publisher Link]

[12] S. Palanivel Rajan, and C. Vivek, "Analysis and Design of Microstrip Patch Antenna for Radar Communication," *Journal of Electrical Engineering & Technology*, vol. 14, pp. 923-929, 2019. [CrossRef] [Google Scholar] [Publisher Link]

[13] Md. Abdullah-Al-Mamun, Sham Datto, and Md. Shahinur Rahman, "Performance Analysis of Rectangular, Circular and Elliptical Shape Microstrip Patch Antenna Using Coaxial Probe Feed," *2nd International Conference on Electrical & Electronic Engineering (ICEEE)*, Rajshahi, Bangladesh, pp. 1-4, 2017. [CrossRef] [Google Scholar] [Publisher Link]

[14] Saqib Hussain et al., "Design of Wearable Patch Antenna for Wireless Body Area Networks," *International Journal of Advanced Computer Science and Applications*, vol. 9, no. 9, pp. 146-151, 2018. [CrossRef] [Google Scholar] [Publisher Link]

[15] Diego Felipe Mona Boada, Eduardo Seiji Sakomura, and Daniel Chagas do Nascimento, "Cavity Model Surrogate-Based Optimization for Electrically Thick Circularly Polarized Rectangular Microstrip Antennas," *AEU - International Journal of Electronics and Communications*, vol. 131, 2021. [CrossRef] [Google Scholar] [Publisher Link]

[16] Kai-Fong Lee, and Kin-Fai Tong, "Microstrip Patch Antennas-Basic Characteristics and Some Recent Advances," *Proceedings of the IEEE*, vol. 100, no. 7, pp. 2169-2180, 2012. [CrossRef] [Google Scholar] [Publisher Link]

[17] Umar Musa et al., "Bandwidth Enhancement of Millimeter-Wave Microstrip Patch Antenna Array for 5G Mobile Communication Networks," *Bulletin of Electrical Engineering and Informatics*, vol. 12, no. 4, pp. 2203-2211, 2023. [CrossRef] [Google Scholar] [Publisher Link]

[18] B. Nataraj, and K.R. Prabha, "Analysis of Various Microstrip Patch Antenna Designs for 5G Applications," *First International Conference on Electrical, Electronics, Information and Communication Technologies (ICEEICT)*, Trichy, India, pp. 01-04, 2022. [CrossRef] [Google Scholar] [Publisher Link]

[19] Zakyra Imana Othman et al., "Microstrip Patch Antenna Design with Artificial Magnetic Conductor (AMC) at 26 GHz," *Journal of Electronic Voltage and Application*, vol. 3, no. 1, pp. 105-113, 2022. [Google Scholar] [Publisher Link]

[20] Surendran Subramanian et al., "Multiband High Gain Microstrip Patch Antenna at Ka Band (26 GHz)," *Journal of Advanced Research in Dynamical and Control Systems*, vol. 11, no. 12-special issue, pp. 667-673, 2019. [CrossRef] [Google Scholar] [Publisher Link]

[21] G. Varshitha, and Bhuvaneswari Balachander, "Design and Performance of Hexagonal Patch Antenna Using Porcelain Dielectric Material in Comparison with Lead Glass Dielectric Material," *11th International Conference on System Modeling & Advancement in Research Trends (SMART)*, Moradabad, India, pp. 618-623, 2022. [CrossRef] [Google Scholar] [Publisher Link]

[22] Noor Hidayah Mohd Yunus et al., "Investigation of Micromachined Antenna Substrates Operating at 5GHz for RF Energy Harvesting Applications," *Micromachines*, vol. 10, no. 2, 2019. [CrossRef] [Google Scholar] [Publisher Link]

[23] Asif Ali et al., "Design and Simulation of a Rectangular E-Shaped Microstrip Patch Antenna for RFID Based Intelligent Transportation," *International Journal of Advanced Computer Science and Applications*, vol. 9, no. 4, pp. 165-169, 2018. [CrossRef] [Google Scholar] [Publisher Link]

[24] Mohammed E. Yassin et al., "Single-Fed 4G/5G Multiband 2.4/5.5/28 GHz Antenna," *IET Microwaves, Antennas & Propagation*, vol. 13, no. 3, pp. 286-290, 2019. [CrossRef] [Google Scholar] [Publisher Link]